Supplementary Information:

Food web structure and intraguild predation affect ecosystem functioning in an established plankton model

A. E. Friederike Prowe[1*], Bei Su[2,3,4*], Jens C. Nejstgaard[5], and Markus Schartau[1]

[1] *GEOMAR Helmholtz Centre for Ocean Research Kiel, Kiel, Germany*

[2] *Institute of Marine Science and Technology, Shandong University, Qingdao, China*

[3] *Southern Marine Science and Engineering Guangdong Laboratory, Zhuhai, China*

[4] *School of Environmental Sciences, University of Liverpool, UK*

[5] *Leibniz Institute of Freshwater Ecology and Inland Fisheries (IGB), Stechlin, Germany*

[*] *Corresponding authors: fprowe@geomar.de, bei.su@sdu.edu.cn*

Figure S1: Minimum microbial food web model as applied by Thingstad et al. (2007, grey arrows) describing fluxes between phosphate (P), bacteria (B), autotrophic flagellates (A), diatoms (D), heterotrophic flagellates (H), ciliates (C) and mesozooplankton (M) in a double-pentagon food web. A newly introduced variable resolves untraced organic phosphorus (UOP*) accumulating in the mesocosms, which in the model originates from unassimilated ingestion, and its remineralisation (orange arrows). In the figure, this one compartment is indicated by several orange boxes for graphical reasons. Dark dashed arrows mark trophic interactions examined in this study.

1 Model setup

The aim of this study is to analyse potential effects of food web structure on ecosystem functioning in a model simulating in the plankton community observed during the PAME-I mesocosm experiment (Larsen et al., 2015). Different food web structures are realised by adding trophic links to an established model of plankton communities, the Minimum microbial food web model (Thingstad et al., 2007, Fig. S1). Model conversion factors are taken from the Larsen et al. (2015, Table S1), and measurement uncertainties are estimated from plausible detection limits of the methods applied, as they are not given in the original publication. Initial values are taken from the observations (Table S2).

Table S1: Estimated error σ (measurement uncertainty) of the observations as used in the cost function and conversion factors to convert to model units.

Variable	Meaning	Conversion factor	Measurement uncertainty	σ	Unit
P	phosphate		near detection limit	20	$\mathrm{nmolP\,L^{-1}}$
B	bacteria	$3.33 \times 10^{-8} \mathrm{nmolP\,cell^{-1}}$	$5 \times 10^5 \mathrm{\,cells\,mL^{-1}}$	16.65	$\mathrm{nmolP\,L^{-1}}$
A	autotrophic nanoflagellates	$47.2 \mathrm{\,nmolP\,ugChl\,a^{-1}}$	Chl a: 10%	0.1 x obs	$\mathrm{nmolP\,L^{-1}}$
H	heterotrophic nanoflagellates	$4 \times 10^{-4} \mathrm{nmolP\,cell^{-1}}$	$10^2 \mathrm{\,cells\,mL^{-1}}$	40	$\mathrm{nmolP\,L^{-1}}$
D	diatoms	$47.2 \mathrm{\,nmolP\,ugChl\,a^{-1}}$	Chl a: 10%	0.1 x obs	$\mathrm{nmolP\,L^{-1}}$
C	ciliates	$1 \times 10^{-1} \mathrm{nmolP\,cell^{-1}}$	$10^3 \mathrm{\,cells\,mL^{-1}}$	10	$\mathrm{nmolP\,L^{-1}}$
M	other copepods (mostly calanoids)	$50 \mathrm{molC\,molP^{-1}}$	10%	0.1 x obs	$\mathrm{nmolP\,L^{-1}}$

2 Food web configurations

This study compares four basic food web configurations (Fig. S1), which are further combined in all possible ways to yield eight food webs of different complexity (Tab. S3).

Underlying the analysis presented in the main text are four basic food web configurations (Table S3):

1. *control*: the original Minimum model food web published by Thingstad et al. (2007), without a trophic link between diatoms and ciliates.

2. *d2c*: the food web of Larsen et al. (2015), with ciliates feeding on diatoms (the D-C link).

3. *ig*: the *control* food web with additional (intraguild) predation of ciliates on their own compartment.

4. *thd*: the *control* food web with threshold feeding of copepods on diatoms, but not for feeding on ciliates.

A feeding link between diatoms and ciliates (Larsen et al., 2015) can be justified by the observation of small-celled diatoms in PAME-I that are within the prey size range of microzooplankton. Here, we

3

Table S2: Fixed parameter values of the modified (this study) and original (Larsen et al., 2015, their fig. 8) Minimum model applied to the mesocosm observations of the PAME-I experiment.

Parameter	Meaning	Larsen et al. (2015)	this study	Unit
Fixed:				
Y_H	H yield on B	0.3	0.4	$\mathrm{nmolP\,nmolP^{-1}}$
Y_C	Ciliate yield on A and H	0.2	0.4	$\mathrm{nmolP\,nmolP^{-1}}$
Y_M	M yield on C and D	0.15	0.1	$\mathrm{nmolP\,nmolP^{-1}}$
— IC & forcing – PAME-I:				
P_0	Initial biomass of P	0.66[1]	79.00	$\mathrm{nmolP\,L^{-1}}$
B_0	Initial biomass of B	58.33[1]	73.66	$\mathrm{nmolP\,L^{-1}}$
A_0	Initial biomass of A	65.71[1]	28.70	$\mathrm{nmolP\,L^{-1}}$
D_0	Initial biomass of D	7.80[1]	11.33	$\mathrm{nmolP\,L^{-1}}$
H_0	Initial biomass of H	35.00[1]	32.40	$\mathrm{nmolP\,L^{-1}}$
C_0	Initial biomass of C	52.50[1]	64.26	$\mathrm{nmolP\,L^{-1}}$
M_0	Initial biomass of M	35.00	13.62	$\mathrm{nmolP\,L^{-1}}$
P_t	Total P in microbial part of the food web	220	220	$\mathrm{nmolP\,L^{-1}}$
E_{P_i}	Experimental input rate of P	4.17	5.96	$\mathrm{nmolP\,L^{-1}\,h^{-1}}$

[1] Initial values in Larsen et al. (2015) are calculated assuming the model system to be in steady state ($\partial X/\partial t = 0$ for $X = P, B, A, D, H, C, M$).

keep the established name of the compartment, "ciliates (C)", to denote all larger microzooplankton in contrast to the smaller heterotrophic nanoflagellates, without excluding other unquantified groups such as dinoflagellates or rotifers.

During the experiments, two distinct size classes of ciliates were observed, either notably larger or smaller than 30 μm in body size (Jens Nejstgaard, pers. obs.). These size classes are grazed by the dominant mesozooplankton, copepods, at very different rates (Nejstgaard et al., 2001*b,a*). Although microzooplankton were counted with a FlowCam and species were not reported in Larsen et al. (2015), we suggest that the smaller microzooplankton may have been a food source for at least some of the larger ciliates. As

ciliates of $> 30\ \mu m$ body size can feed on relatively large prey including other ciliates (e.g., Dolan and Coats, 1991; Diehl and Feissel, 2001; Vasseur and Fox, 2009) and IGP for microzooplankton has been repeatedly reported (e.g., references in Franzé and Modigh, 2013), we consider IGP as plausible trophic link in configuration *ig*.

In the *thd* configuration we consider a feeding threshold for mesozooplankton feeding on diatoms motivated by the dominance of large calanoid copepods in the mesocosms. *Calanus* spp. is generally expected to use a feeding current when feeding on small immotile prey such as smaller diatoms (Price and Paffenhöfer, 1986).The related energy expense and predation risk may cause feeding to stop below a certain threshold prey concentration (Kiørboe and Jiang, 2013). In contrast, for large motile prey like ciliates, theory suggests an ambush feeding strategy with low predation risk and metabolic cost, thus not resulting in any feeding threshold (Kiørboe et al., 2018).

The above three configuration options are further combined in all possible ways (cf. Table S3):

5. *igthd*: allowing threshold feeding of copepods on diatoms (configuration *thd*) in the configuration *ig* with IGP of ciliates.

6. *igd2c*: combining food webs *ig* and *d2c* allowing grazing of ciliates on diatoms and themselves.

7. *d2cthd*: allowing threshold feeding of copepods on diatoms in configuration *d2c* where ciliates may feed on diatoms.

8. *igd2cthd*: most complex food web with the D-C link, IGP of ciliates and threshold feeding of copepods on diatoms.

3 The modified Minimum Model

In order to resolve and compare the different food web configurations detailed above, the original model equations are modified in two ways. Additional trophic links are formulated according to the existing model equations and defined using configurative parameters ($\mathbf{c_2}$, $\mathbf{c_3}$, $\mathbf{D_{th}}$; Tables S5, S6) that allow selection of each trophic link individually. Furthermore, an additional state variable UOP* is introduced to allow mass-conserving (in terms of total phosphorus) quantitative simulations of the observations.

3.1 Standard model variables and their equations

Bacteria:

$$\frac{\partial B}{\partial t} = [\mu_B - I_H H]\, B \quad , \qquad \mu_B = \frac{\alpha_B \mu_B P}{\mu_B + \alpha_B P} \tag{S1}$$

ANFs:

$$\frac{\partial A}{\partial t} = [\mu_A - I_C C]\, A \quad , \qquad \mu_A = \frac{\alpha_A \mu_A P}{\mu_A + \alpha_A P} \tag{S2}$$

Diatoms:

$$\frac{\partial D}{\partial t} = [\mu_D - \mathbf{c_2} I_C C]\, D - (1 - \mathbf{c_2}) I_M M \hat{D} \quad , \qquad \mu_D = \frac{\alpha_D \mu_D P}{\mu_D + \alpha_D P} \tag{S3}$$

$$\hat{D} = max(D - \mathbf{D_{th}}, 0) \tag{S4}$$

HNFs:

$$\frac{\partial H}{\partial t} = [Y_H I_H B - I_C C]\, H \quad , \qquad I_H = \frac{\alpha_H \mu_H}{\mu_H + Y_H \alpha_H B} \tag{S5}$$

Ciliates:

$$\frac{\partial C}{\partial t} = [Y_C I_C (A + H + \mathbf{c_2} D + \mathbf{c_3} C)]\, C - c_1 I_M M C - \mathbf{c_3} I_C C^2 \tag{S6}$$

$$I_C = \frac{\alpha_C \mu_C}{\mu_C + Y_C \alpha_C (H + A + \mathbf{c_2} D + \mathbf{c_3} C)} \tag{S7}$$

6

Mesozoo:

$$\frac{\partial M}{\partial t} = Y_M I_M \left[(1 - \mathbf{c_2})\hat{D} + c_1 C\right] M \quad , \qquad I_M \quad = \frac{\alpha_M \mu_M}{\mu_M + Y_M \alpha_M \left[(1 - \mathbf{c_2})\hat{D} + c_1 C\right]} \tag{S8}$$

Phosphate:

$$\frac{\partial P}{\partial t} = E_{P_i} - \mu_B B - \mu_A A - \mu_D D + R\,(unassim.grazing) \tag{S9}$$

3.2 Unresolved organic P accumulation

A mesocosm is a closed system and the continuous addition of PO_4^{3-} causes total phosphorus (TP) to accumulate. Such accumulation of TP is not reflected by the available observations, as the sum of measured PO_4^{3-} and biomass of all biological compartments underestimates the TP increase expected from additions (Fig. S2a). This indicates a net sink of phosphorus unresolved by the observations.

A new variable UOP^* is introduced to collect the unresolved (organic) P pool accumulating in the mesocosms outside the measured compartments. The UOP^* reflects wall growth and sedimentation in the mesocosm enclosures. In the mesocoms, TP is estimated from the documented PO_4^{3-} addition rate ($E_{P_i} t_i$) and the total P in observed variables at the start of the experiment (P_t).

$$TP_i = E_{P_i} t_i + P_t \quad , \quad P_t = P_0 + B_0 + A_0 + D_0 + H_0 + C_0 + M_0 \tag{S10}$$

The observed UOP^* is then estimated from the difference between TP and the measurements of all variables at four points in time t_i, when all variables were measured simultaneously (Fig. S2b).

$$UOP^*{}_i = TP_i - (P_i + B_i + A_i + D_i + H_i + C_i + M_i) \tag{S11}$$

This estimate reveals a substantial overestimation of the observed total P content in simulations assuming instant remineralisation and no accumulation of UOP^* (Fig. S2a, dashed line).

In the model, UOP^* is fed by the unassimilated grazing fraction (Eq. S12). Other processes, e.g., aggregation of phytoplankton material, are not resolved for the sake of simplicity. UOP^* is remineralised to

7

PO_4^{3-} with rate R and may therefore contribute to regenerated production.

$$\frac{\partial \text{UOP}^*}{\partial t} = (1-R)[\ \underbrace{(1-Y_H)I_H BH}_{unassim.Hgrazing} + \underbrace{(1-Y_C)I_C(A+H+\mathbf{c_2}D+\mathbf{c_3}C)C}_{unassim.Cgrazing} \qquad \text{(S12)}$$

$$+ \underbrace{(1-Y_M)I_M\left[(1-\mathbf{c_2})\hat{D}+c_1 C\right]M}_{unassim.Mgrazing}\ ]$$

72 The model fit to the estimated UOP^* is considered when optimising the model against the observation-

73 based estimates at times when all variables were measured. This approach proves essential for assuring

74 identical constraints with respect to mass conservation for all model setups.
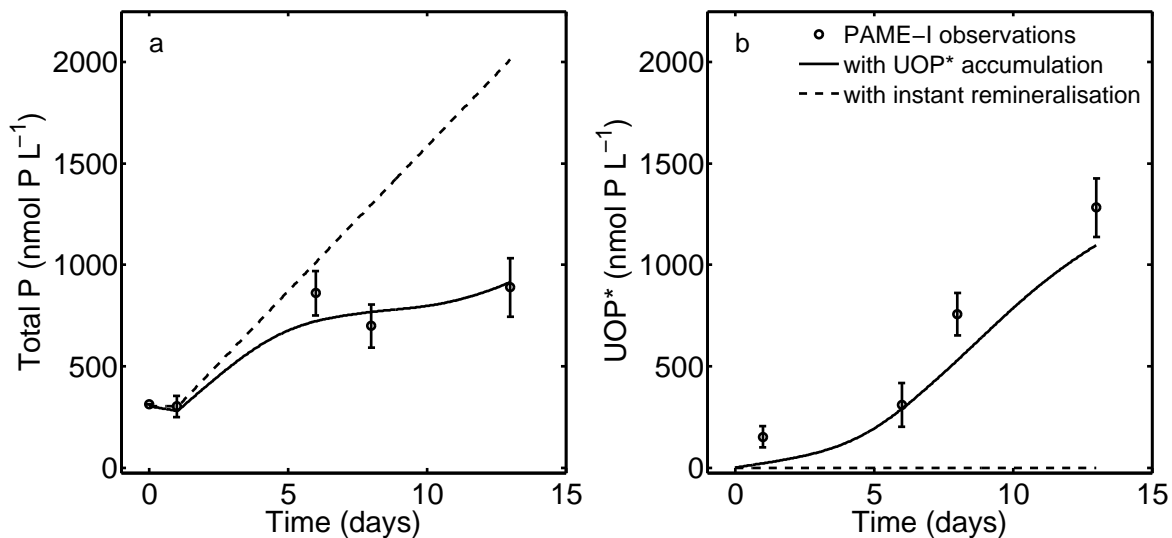
Figure S2: Total phosphorus inventory in originally resolved model variables (as sum of P and the biomass of bacteria (B), autotrophic flagellates (A), diatoms (D), heterotrophic flagellates (H), ciliates (C) and mesozooplankton (M); a), and accumulating untraced organic phosphorus (UOP*; b) derived from the observations (circles) and in simulations with the *d2c* food web assuming accumulation and partial remineralisation of UOP* (solid line) or no accumulation and instant remineralisation of UOP* (dashed line). The UOP* is calculated as difference between the measured phosphorus (circles) and total phosphorus from additions (which equals total phosphorus when assuming instant remineralisation), imposing mass conservation (Eqs. S10, S11). The legend for both panels is shown only in panel b.

4 Model optimisation

4.1 Optimisation details

The food web configurations represent different levels of complexity in terms of numbers of parameters (Table S3). Forcing parameters like the PO_4^{3-} addition rate, the initial TP in the microbial part of the food web, and the initial values remain fixed (Table S2). In preliminary optimisations the growth efficiency or yield values (Y_H, Y_C, Y_M) were always optimised to their upper ($Y_H = Y_C = 0.4$) and lower ($Y_M = 0.1$) limits of physiologically reasonable values according to literature and expert knowledge, and these parameters are not optimised.

The optimisation algorithm used is the Matlab version of the Covariance Matrix Adaptation Evolution Strategy algorithm (CMA-ES; Hansen and Ostermeier, 2001). CMA-ES generates random combinations of values for the parameters to be optimised. For each combination, the model results are evaluated against the observational data, using a cost function that quantifies the model-data misfit. As preparation, the optimisation setup is tested by treating model results of a reference solution as pseudo-data (identical twin data). This twin experiment allows to consolidate the overall performance of the optimisation approach and introduce refinements, in this case the implementation of UOP* in the cost function. The cost function J is calculated as

$$J = \sum_{i=1}^{N_t} \sum_{j=1}^{N_y} \frac{\left(y_{ij} - \eta_{ij}(x)\right)^2}{\sigma_{ij}^2} \tag{S13}$$

with observations y_{ij} for $y = P, B, A, D, H, C, M, UOP^*$ and model data η_{ij} at times $i = 1, \ldots, t$ of the observations. σ is taken as the measurement uncertainty of the observations y. Since observational errors are not reported in the original publication, values of σ are set to reflect minimal yet plausible observational error assumptions (e.g. a detection limit for PO_4^{3-}; Table S1). The identification of the cost function's minimum is tantamount to having found maximum likelihood parameter estimates for a given

10

model.

For the optimisation, the CMA-ES determines a population size according to $4 + ln(3*N_p)$ with N_p being the number of parameters to be optimised (Table S3). The optimisation algorithm requires between about 4400 to 9400 iterations, depending on model configuration before reaching stagnation of the cost function values.

Table S3: Food web configurations with their respective model parameters, complexity (no. of optimised parameters) and optimiser settings. Further details regarding parameters, their meaning and values is given in Tables S5 and S6.

Simulation	Food web	configurative parameters			No. of parameters		Population	No. of
		c_2	c_3	D_{th}	total	optimised	Size	iterations
control	as used in Thingstad et al. (2007)	0	0	0	20	14	11	6212
d2c	as in Larsen et al. (2015) with C feeding on D	>0	0	0	21	15	12	4465
ig	C feeding on themselves (intraguild grazing)	0	>0	0	21	15	12	6136
thd	threshold feeding of M on D	0	0	>0	21	15	12	7744
igd2c	C feeding on D and on themselves	>0	>0	0	22	16	12	7973
igthd	C feeding on themselves and threshold feeding of M on D	0	>0	>0	22	16	12	6399
d2cthd	C feeding on D and threshold feeding of M on D	>0	0	>0	22	16	12	5862
igd2cthd	full model	>0	>0	>0	23	17	12	9366

In order to identify a model configuration of minimum complexity that captures the essential dynamics involved in the microbial food web, the F score (Ward et al., 2013; Schartau et al., 2017) can be applied to assess the models' performances against each other. The F score is calculated as

$$F = \frac{LRT}{J(\text{complex})} \frac{df}{N_p(\text{complex}) - N_p(\text{simple})} \tag{S14}$$

where $LRT = J(\text{simple}) - J(\text{complex})$ represents a the logarithm of a Likelihood ratio (likelihood ratio test). $N_p(\text{complex})$ and $N_p(\text{simple})$ are the numbers of optimised parameters (Table S3) of the most complex and the simpler model versions, respectively, and $df = N_{obs} - N_p(\text{complex})$ denotes the

11

degrees of freedom of the most complex model. Eq. (S14) allows to evaluate whether an increase in the minimum value of the cost function (Eq. S13) remains tolerable or insignificant within some limits ΔJ, relative to the minimum of the most complex model. These limits are determined as thresholds based on the F-distribution with the degree of freedom of the most complex model (here *igd2cthd* with N_p=17) and of the simpler models, respectively.

In such an approach, the probability distributions of the cost functions' minima are treated as χ^2-distributions. Thus, the LRT can be interpreted as the ratio of two χ^2-distributions with two different degrees of freedom, with $df_1 = N_p(\text{complex}) - N_p(\text{simple})$ and df as above. While N_p can differ between individual model versions the number of observational data points remains constant ($N_{obs} = 55$). An F score below or equal to a threshold value identifies the best most parsimonious model. The threshold values of $F(df_1, df)$ were computed for the $\alpha = 0.05$ confidence level. For the main text, the four configurations with best fit to observations (lowest cost function value J) are selected.

Table S4: Cost function values J, F score (Eq. S14) and Threshold F value for $\alpha = 0.05$ for food webs of different complexity (N_p number of optimised parameters) for the reference configuration *igd2cthd*.

Simulation	Food web	N_p	J	F score	Threshold F
control	as used in Thingstad et al. (2007)	14	528.15	7.83	2.85
ig	C feeding on themselves (intraguild grazing)	15	454.20	8.51	3.24
d2c	as in Larsen et al. (2015) with C feeding on D	15	458.99	8.01	3.24
thd	threshold feeding of M on D	15	603.83	11.53	3.24
igthd	C feeding on themselves and threshold feeding of M on D	16	554.67	18.09	4.02
d2cthd	C feeding on D and threshold feeding of M on D	16	517.37	14.32	4.02
igd2c	C feeding on D and on themselves	16	376.78	0.10	4.02
igd2cthd	full model	17	375.80	–	–

4.2 Optimised parameter values

Table S5: Parameters of the optimised MMFW model simulations presented in the main text.

Parameter	Meaning	Larsen et al. (2015)	igd2c	d2c	ig	control	literature range	Unit
				Value				Unit
Optimised:								
α_B	B affinity for P	8×10^{-2}	9.29×10^{-2}	1.89×10^{-4}	2.05×10^{-4}	1.94×10^{-4}	[1] 3.31×10^{-6}–9.29×10^{-2}	$\mathrm{L\,nmolP^{-1}\,h^{-1}}$
α_A	A affinity for P	4×10^{-2}	3.95×10^{-4}	5.84×10^{-4}	7.71×10^{-4}	4.04×10^{-4}	[2] 1.01×10^{-5}–1.57×10^{-2}	$\mathrm{L\,nmolP^{-1}\,h^{-1}}$
α_D	D affinity for P	3×10^{-2}	5.62×10^{-4}	4.73×10^{-4}	4.56×10^{-4}	3.96×10^{-4}	[2] 2.05×10^{-5}–7.43×10^{-3}	$\mathrm{L\,nmolP^{-1}\,h^{-1}}$
α_H	H clearance rate for B	1.5×10^{-3}	6.17×10^{-4}	4.58×10^{-4}	4.84×10^{-4}	4.52×10^{-4}	[3] 3.3×10^{-5}–2.6×10^{-3}	$\mathrm{L\,nmolP^{-1}\,h^{-1}}$
α_C	C clearance rate for A and H	5×10^{-4}	3.97×10^{-4}	1.70×10^{-4}	1.70×10^{-4}	1.70×10^{-4}	[3] 1.7×10^{-4}–1.0×10^{-2}	$\mathrm{L\,nmolP^{-1}\,h^{-1}}$
α_M	M clearance rate for C and D	1.5×10^{-4}	2.8×10^{-3}	2.8×10^{-3}	1.91×10^{-3}	1.55×10^{-3}	[3] 8.3×10^{-6}–2.82×10^{-3}	$\mathrm{L\,nmolP^{-1}\,h^{-1}}$
μ_B	Maximum growth rate B	2.50×10^{-2}	2.60×10^{-2}	2.40×10^{-2}	2.40×10^{0}	2.40×10^{0}	[1] 1.35×10^{-2}–2.4×10^{0}	$\mathrm{h^{-1}}$
μ_A	Maximum growth rate A	5.4×10^{-2}	1.00×10^{-1}	3.59×10^{-2}	3.39×10^{-2}	4.53×10^{-2}	[2] 7.9×10^{-3}–1.0×10^{-1}	$\mathrm{h^{-1}}$
μ_D	Maximum growth rate D	6.3×10^{-2}	1.10×10^{-1}	9.58×10^{-2}	1.10×10^{-1}	1.10×10^{-1}	[2] 9.5×10^{-3}–1.1×10^{-1}	$\mathrm{h^{-1}}$
μ_H	Maximum growth rate H	1.0×10^{-1}	8.60×10^{-2}	8.60×10^{-2}	8.60×10^{-2}	8.60×10^{-2}	[3] 9.7×10^{-3}–8.6×10^{-2}	$\mathrm{h^{-1}}$
μ_C	Maximum growth rate C	5×10^{-2}	2.26×10^{-2}	4.57×10^{-2}	3.46×10^{-2}	2.46×10^{-2}	[3] 3.9×10^{-3}–4.6×10^{-2}	$\mathrm{h^{-1}}$
μ_M	Maximum growth rate M	6.25×10^{-3}	1.00×10^{-2}	8.90×10^{-3}	1.20×10^{-2}	1.33×10^{-2}	[3] 6.2×10^{-4}–1.8×10^{-2}	$\mathrm{h^{-1}}$
R	Remineralization fraction of UOP*	1.00×10^{0}	5.13×10^{-1}	3.10×10^{-1}	3.03×10^{-1}	1.84×10^{-1}		
— configurative:								
c_1	M selective factor for C relative to D	2	3.03×10^{-2}	9.84×10^{-2}	2.00×10^{-10}	2.00×10^{-4}		
$\mathbf{c_2}$	C clearance rate for D as fraction of α_C	5.50×10^{-1}	6.90×10^{-1}	3.93×10^{-1}	–	–		
	α_M for D reduced by factor $(1-\mathbf{c_2})$							
$\mathbf{c_3}$	C intraguild clearance rate as fraction of α_C	–	2.00×10^{-1}	–	8.40×10^{-2}	–		

[1] Button (1998) converted using wet weight to g C conversion factors therein and $106\ \mathrm{nmolC\,nmolP^{-1}}$

[2] Edwards et al. (2015) using $16\ \mathrm{nmolN\,nmolP^{-1}}$, maximum growth rates converted to $7.5°C$ using Q_{10}=1.53 (Kremer et al., 2017)

[3] Kiørboe and Hirst (2014) with temperature correction to $7.5°C$ using Q_{10}=2.8 (Hansen et al., 1997)

Table S6: Parameters of the optimised MMFW models: additional simulations not presented in detail in the main text.

Parameter	Meaning	Value							Unit
		Larsen et al. (2015)	igd2cthd	igd2c	d2cthd	igthd	thd	literature range	
Optimised:									
α_B	B affinity for P	8×10^{-2}	9.29×10^{-2}	9.29×10^{-2}	1.93×10^{-4}	2.04×10^{-4}	2.11×10^{-4}	[1] 3.31×10^{-6}–9.29×10^{-2}	$\mathrm{L\,nmolP^{-1}\,h^{-1}}$
α_A	A affinity for P	4×10^{-2}	4.06×10^{-4}	3.95×10^{-4}	3.13×10^{-4}	5.58×10^{-4}	2.55×10^{-4}	[2] 1.01×10^{-5}–1.57×10^{-2}	$\mathrm{L\,nmolP^{-1}\,h^{-1}}$
α_D	D affinity for P	3×10^{-2}	5.92×10^{-4}	5.62×10^{-4}	2.87×10^{-4}	1.56×10^{-4}	1.41×10^{-4}	[2] 2.05×10^{-5}–7.43×10^{-3}	$\mathrm{L\,nmolP^{-1}\,h^{-1}}$
α_H	H clearance rate for B	1.5×10^{-3}	6.14×10^{-4}	6.17×10^{-4}	4.54×10^{-4}	4.71×10^{-4}	4.63×10^{-4}	[3] 3.3×10^{-5}–2.6×10^{-3}	$\mathrm{L\,nmolP^{-1}\,h^{-1}}$
α_C	C clearance rate for A and H	5×10^{-4}	1.44×10^{-4}	3.97×10^{-4}	1.70×10^{-4}	1.70×10^{-4}	1.70×10^{-4}	[3] 1.7×10^{-4}–1.0×10^{-2}	$\mathrm{L\,nmolP^{-1}\,h^{-1}}$
α_M	M clearance rate for C and D	1.5×10^{-4}	2.8×10^{-3}	2.8×10^{-3}	2.82×10^{-3}	2.82×10^{-3}	2.82×10^{-3}	[3] 8.3×10^{-6}–2.82×10^{-3}	$\mathrm{L\,nmolP^{-1}\,h^{-1}}$
μ_B	Maximum growth rate B	2.50×10^{-2}	2.62×10^{-2}	2.60×10^{-2}	2.40×10^{0}	2.40×10^{-2}	2.40×10^{0}	[1] 1.35×10^{-2}–2.4×10^{0}	$\mathrm{h^{-1}}$
μ_A	Maximum growth rate A	5.4×10^{-2}	1.00×10^{-1}	1.00×10^{-1}	6.12×10^{-2}	3.90×10^{-2}	1.00×10^{-1}	[2] 7.9×10^{-3}–1.0×10^{-1}	$\mathrm{h^{-1}}$
μ_D	Maximum growth rate D	6.3×10^{-2}	1.11×10^{-1}	1.10×10^{-1}	6.85×10^{-2}	5.44×10^{-2}	1.10×10^{-1}	[2] 9.5×10^{-3}–1.1×10^{-1}	$\mathrm{h^{-1}}$
μ_H	Maximum growth rate H	1.0×10^{-1}	8.60×10^{-2}	8.60×10^{-2}	8.60×10^{-2}	8.60×10^{-2}	7.72×10^{-2}	[3] 9.7×10^{-3}–8.6×10^{-2}	$\mathrm{h^{-1}}$
μ_C	Maximum growth rate C	5×10^{-2}	2.21×10^{-2}	2.26×10^{-2}	4.60×10^{-2}	3.09×10^{-2}	2.25×10^{-2}	[3] 3.9×10^{-3}–4.6×10^{-2}	$\mathrm{h^{-1}}$
μ_M	Maximum growth rate M	6.25×10^{-3}	1.03×10^{-2}	1.00×10^{-2}	1.80×10^{-2}	1.80×10^{-2}	1.80×10^{-2}	[3] 6.2×10^{-4}–1.8×10^{-2}	$\mathrm{h^{-1}}$
R	Remineralization fraction of UOP*	1.00×10^{0}	5.19×10^{-1}	5.13×10^{-1}	2.17×10^{-1}	4.14×10^{-2}	1.00×10^{-6}		
— configurative:									
c_1	M selective factor for C relative to D	2.00×10^{0}	1.83×10^{-2}	3.03×10^{-2}	8.37×10^{-2}	2.00×10^{-4}	2.00×10^{-4}		
$\mathbf{c_2}$	C clearance rate for D as fraction of α_C α_M for D reduced by factor $(1 - \mathbf{c_2})$	5.50×10^{-1}	6.81×10^{-1}	6.90×10^{-1}	6.47×10^{-1}	–	–		
$\mathbf{c_3}$		–	2.2×10^{-1}	2.00×10^{-1}	–	6.85×10^{-2}	–		
$\mathbf{D_{th}}$		–	3.50×10^{-4}	–	$1.11 \times 10^{+2}$	$6.49 \times 10^{+1}$	$6.43 \times 10^{+1}$		$\mathrm{nmolP\,L^{-1}}$

[1] Button (1998) converted using wet weight to g C conversion factors therein and $106\ \mathrm{nmolC\,nmolP^{-1}}$

[2] Edwards et al. (2015) using $16\ \mathrm{nmolN\,nmolP^{-1}}$, maximum growth rates converted to 7.5°C using Q_{10}=1.53 (Kremer et al., 2017)

[3] Kiørboe and Hirst (2014) with temperature correction to 7.5°C using Q_{10}=2.8 (Hansen et al., 1997)

5   Trophic transfer efficiency and trophic level

Tropic transfer efficiency is estimated following Kemp et al. (2001) as

$$TTE = \frac{Y_M I_M \left[(1 - \mathbf{c_2})\hat{D} + c_1 C\right] M}{\mu_A A + \mu_D D}$$ (S15)

The trophic level of mesozooplankton (TL_M) is calculated from the fraction of diatom and ciliate inges-

tion relative to total mesozooplankton ingestion (Ulanowicz, 1995).

$$
\begin{aligned}
TL_M &= 1 + 1\frac{I_M(1 - \mathbf{c_2})\hat{D}M}{I_M \left[(1 - \mathbf{c_2})\hat{D} + c_1 C\right] M} + TL_C \frac{I_M c_1 CM}{I_M \left[(1 - \mathbf{c_2})\hat{D} + c_1 C\right] M} \\
&= 1 + 1\frac{(1 - \mathbf{c_2})\hat{D}}{(1 - \mathbf{c_2})\hat{D} + c_1 C} + TL_C \frac{c_1 C}{(1 - \mathbf{c_2})\hat{D} + c_1 C}
\end{aligned}
$$ (S16)

The trophic level of ciliates (TL_C) is calculated analogously, assuming for simplicity that intraguild

predation of ciliates is predation of carnivorous ciliates on herbivorous ciliates only.

$$TL_C = 1 + 1\frac{A + \mathbf{c_2}D}{A + H + \mathbf{c_2}D + \mathbf{c_3}C} + 2\frac{H + \mathbf{c_3}C}{A + H + \mathbf{c_2}D + \mathbf{c_3}C}$$ (S17)
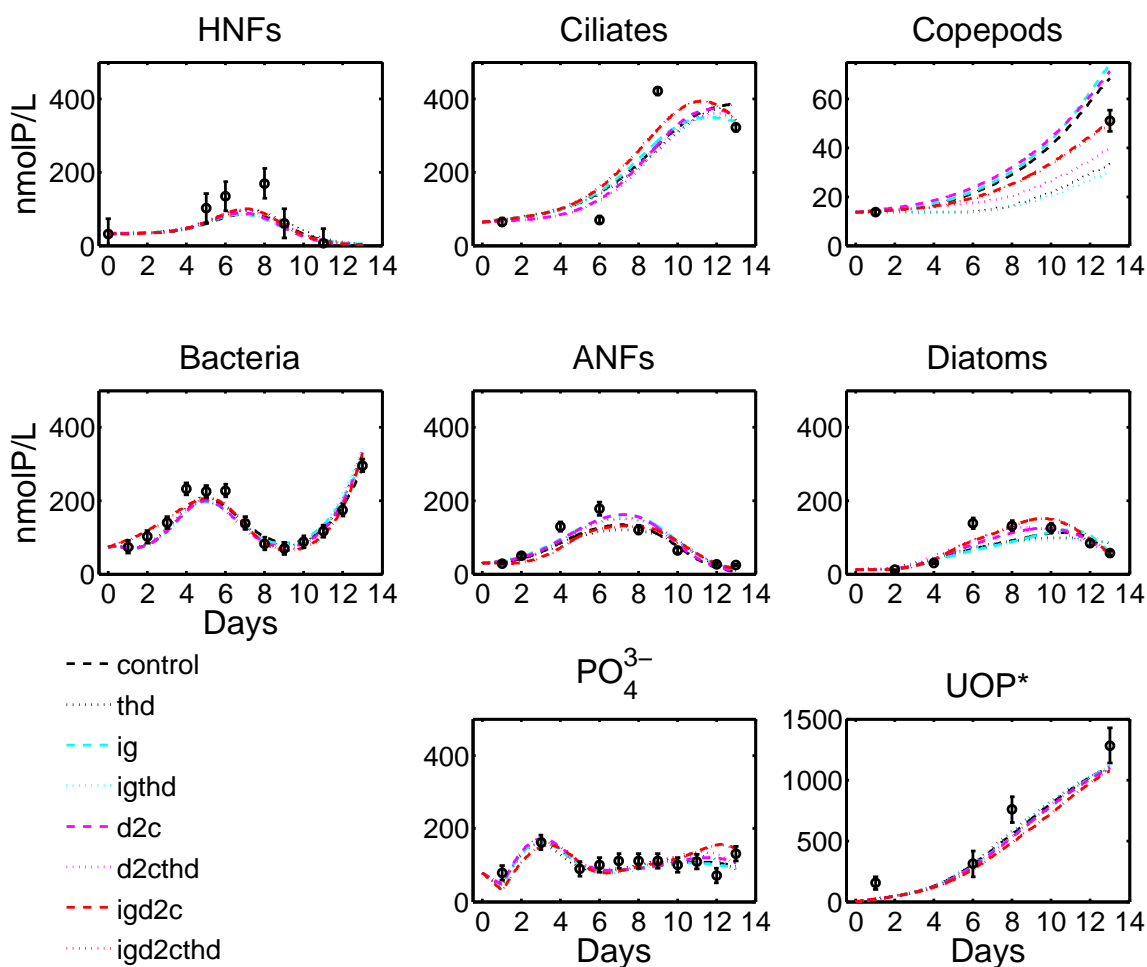
6   Supplementary Results

Figure S3: Simulated dynamics of observed variables during PAME-I and P accumulation for all food webs. P accumulation is deduced from phosphate addition rates minus total P in observed variables (phosphate plus organic P bound in biomass).
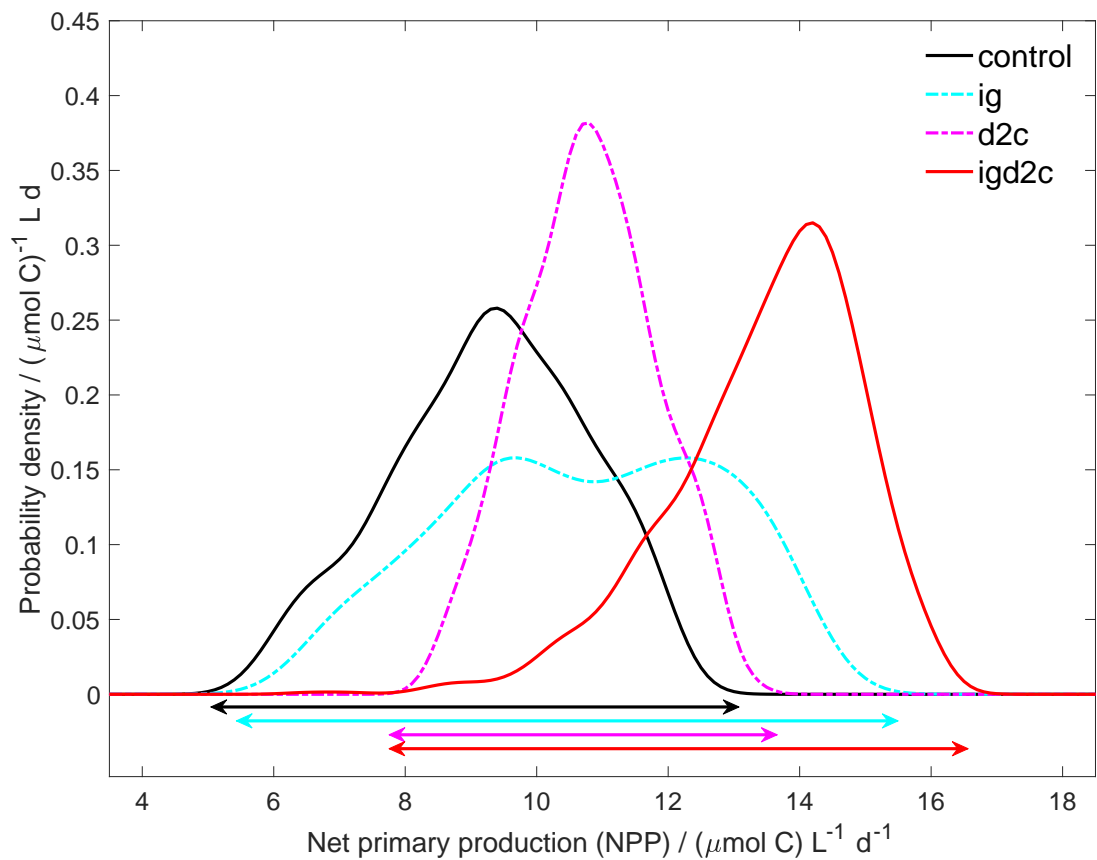
Figure S4: Probability density functions of net primary production in ensemble simulations varying initial conditions randomly by $\pm 20\%$ for selected model configurations.
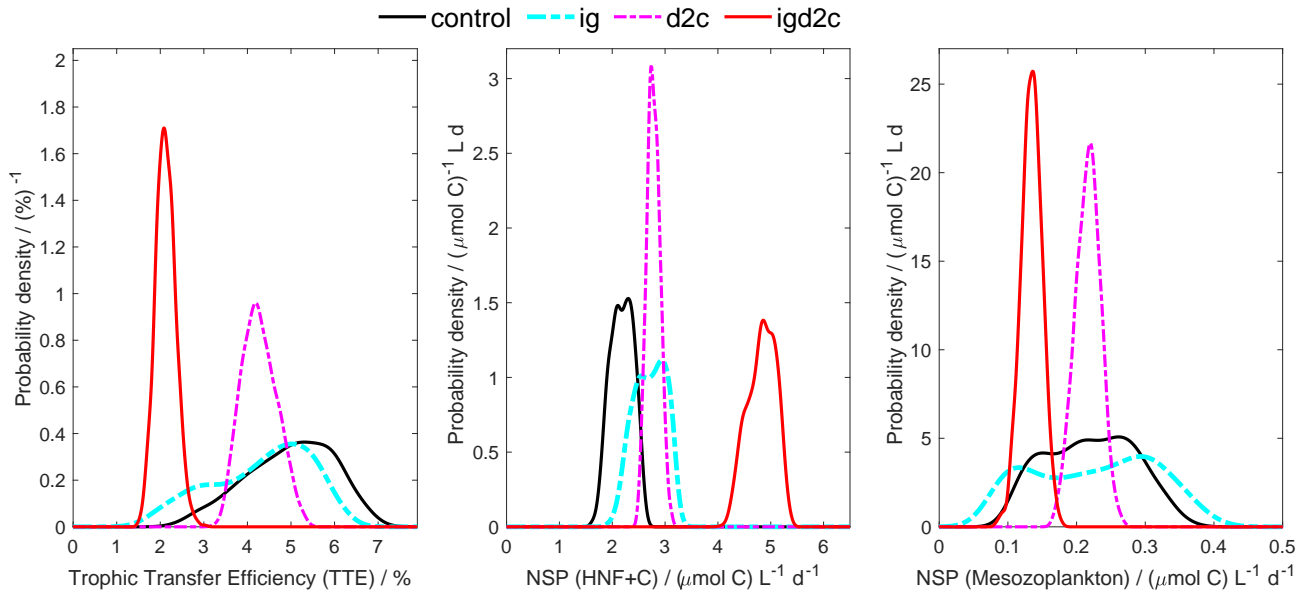
Figure S5: Probability density functions of trophic transfer efficiency (TTE; left) and net secondary production of microzooplankton (NSP_{H+C}; center) and mesozooplankton (NSP_M; right) in an ensemble of simulations varying initial conditions randomly by $\pm 20\%$ for selected model configurations. Chain- and mesh-like food webs are indicated by cold and warm colours, respectively.

References

Button, D. K. 1998. Nutrient uptake by microorganisms according to kinetic parameters from theory as related to cytoarchitecture. Microbiology and Molecular Biology Reviews **62**: 636–+.

Diehl, S., and M. Feissel. 2001. Intraguild prey suffer from enrichment of their resources: a microcosm experiment with ciliates. Ecology **82**.

Dolan, J. R., and D. W. Coats. 1991. A study of feeding in predacious ciliates using prey ciliates labeled with fluorescent microspheres. Journal of Plankton Research **13**: 609–627.

Edwards, K. F., C. A. Klausmeier, and E. Litchman. 2015. Nutrient utilization traits of phytoplankton. Ecology **96**. doi:10.1890/14-2252.1.

Franzé, G., and M. Modigh. 2013. Experimental evidence for internal predation in microzooplankton communities. Mar. Biol. **160**: 3103–3112. doi:10.1007/s00227-013-2298-1.

Hansen, N., and A. Ostermeier. 2001. Completely derandomized self-adaptation in evolution strategies. Evolutionary Computation **9**: 159–195.

Hansen, P. J., P. K. Bjørnsen, and B. W. Hansen. 1997. Zooplankton grazing and growth: Scaling within the 2-2,000-μm body size range. Limnol. Oceanogr. **42**: 687–704.

Kemp, W. M., M. T. Brooks, and R. R. Hood. 2001. Nutrient enrichment, habitat variability and trophic transfer efficiency in simple models of pelagic ecosystmes. meps **223**: 73–87.

Kiørboe, T., and A. G. Hirst. 2014. Shifts in mass scaling of respiration, feeding, and growth rates across life-form transitions in marine pelagic organisms. Am. Nat. **183**: E118–E130. doi:10.1086/675241.

Kiørboe, T., and H. Jiang. 2013. To eat and not be eaten: optimal foraging behaviour in suspension feeding copepods. Journal of the Royal Society Interface **10**. doi:10.1098/rsif.2012.0693.

Kiørboe, T., E. Saiz, P. Tiselius, and K. H. Andersen. 2018. Adaptive feeding behavior and functional responses in zooplankton. Limnology and Oceanography **63**: 308–321. doi:10.1002/lno.10632.

Kremer, C. T., M. K. Thomas, and E. Litchman. 2017. Temperature- and size-scaling of phytoplankton population growth rates: Reconciling the Eppley curve and the metabolic theory of ecology. Limnology and Oceanography **62**: 1658–1670. doi:10.1002/lno.10523.

Larsen, A., J. K. Egge, J. C. Nejstgaard, I. Di Capua, R. Thyrhaug, G. Bratbak, and T. F. Thingstad. 2015. Contrasting response to nutrient manipulation in Arctic mesocosms are reproduced by a minimum microbial food web model. Limnol. Oceanogr. **60**: 360–374. doi:10.1002/lno.10025.

Nejstgaard, J. C., B. H. Hygum, L. J. Naustvoll, and U. Båmstedt. 2001*a*. Zooplankton growth, diet and reproductive success compared in simultaneous diatom- and flagellate-microzooplankton-dominated plankton blooms. Marine Ecology Progress Series **221**: 77–91.

Nejstgaard, J. C., L. J. Naustvoll, and A. Sazhin. 2001*b*. Correcting for underestimation of microzooplankton grazing in bottle incubation experiments with mesozooplankton. Marine Ecology Progress Series **221**: 59–75.

Price, H. J., and G.-A. Paffenhöfer. 1986. Capture of small cells by the copepod *Eucalanus elongatus*. Limnol. Oceanogr. **31**: 189–194. doi:10.4319/lo.1986.31.1.0189.

Schartau, M., et al. 2017. Reviews and syntheses: parameter identification in marine planktonic ecosystem modelling. Biogeosciences **14**: 1647–1701. doi:10.5194/bg-14-1647-2017.

Thingstad, T. F., et al. 2007. Ability of a "minimum" microbial food web model to reproduce response patterns observed in mesocosms manipulated with N and P, glucose, and Si. Journal of Marine Systems **64**: 15–34. doi:10.1016/j.jmarsys.2006.02.009.

164 Ulanowicz, R. E. 1995. Ecosystem trophic foundations: Lindeman exonerata. In B. C. Patten and S. E.

165 Jørgensen (eds.), Ecology: the part-whole relation in ecosystems. Prentice-Hall, Engelwood Cliffs, pp.

166 549–560.

167 Vasseur, D. A., and J. W. Fox. 2009. Phase-locking and environmental fluctuations generate synchrony

168 in a predator-prey community. Nature **460**: 1007–1010. doi:10.1038/nature08208.

169 Ward, B. A., M. Schartau, A. Oschlies, A. P. Martin, M. J. Follows, and T. R. Anderson. 2013. When

170 is a biogeochemical model too complex? Objective model reduction and selection for North Atlantic

171 time-series sites. Progress In Oceanography **116**: 49–65. doi:10.1016/j.pocean.2013.06.002.